Single Lipid Extraction – The Anchoring Strength of Cholesterol in Liquid Ordered and Liquid Disordered Phases

Running Head: Single Cholesterol Extraction from Lipid Membranes

Frank W. S. Stetter[1], Lukasz Cwiklik[2,3*], Pavel Jungwirth[3,4], and Thorsten Hugel[1*]

[1] IMETUM, Physik-Department, Technische Universität München, Munich, Germany

[2] J. Heyrovský Institute of Physical Chemistry, Academy of Sciences of the Czech Republic, v.v.i., Dolejškova 3, 182 23 Prague , Czech Republic

[3] Institute of Organic Chemistry and Biochemistry, Academy of Sciences of the Czech Republic, Flemingovo nam. 2, 16610 Prague, Czech Republic

[4] Department of Physics, Tampere University of Technology, P. O. Box 692, FI-33101 Tampere, Finland

*corresponding authors: lukasz.cwiklik@jh-inst.cas.cz and thugel@mytum.de

ABSTRACT

Cholesterol is important for the formation of microdomains in lipid bilayers and is enriched in the liquid ordered phase. To understand the interactions leading to this enrichment, we developed an AFM based single lipid extraction approach, which allows to determine the anchorage strength of cholesterol in the two phases of a phase separated lipid membrane. As expected, the forces necessary for extracting a single cholesterol molecule from liquid ordered phases are significantly higher than for extracting it from the liquid disordered phases. Interestingly, application of the Bell model shows two energy barriers that correlate with the head and full length of the cholesterol molecule. The resulting lifetimes for complete extraction are 90 s and 11 s in the liquid ordered and liquid disordered phase, respectively. Molecular dynamics simulations of the very same experiment show similar force profiles and indicate that the stabilization of cholesterol in the liquid ordered phase is mainly due to non-polar contacts.

INTRODUCTION

Eukaryotic membranes are quasi two dimensional, highly complex, heterogeneous surfaces consisting of proteins and lipids like phospholipids, sphingolipids, and cholesterol. Cholesterol is particularly import to maintain this heterogeneity since it promotes formation of the so called microdomains (1, 2). These microdomains likely play an important role in signal transduction and sorting of membrane components (3). Furthermore, it has been proposed that microdomains are in a liquid ordered state which is characterized by lipids having a high degree of chain order (as

in the solid state) and at the same time a high lateral mobility of the lipids (as in the liquid disordered state) (4).

Even though the existence of microdomains in cells, which are also often referred to as lipid rafts, is still not conclusively confirmed, they have been intensively studied in model membranes. Typically these model membranes are based on ternary lipid mixtures consisting of a lipid with a low transition temperature like DOPC, a lipid with a high transition temperature like sphingomyelin (SM), and cholesterol. At room temperature a liquid-liquid phase separation is observed, which is characterized by a liquid ordered phase rich in cholesterol and a liquid disordered phase rich in DOPC (5–7).

The different affinity of lipids for different lipid environments is important for such diverse processes as the fusion of vesicles (8), the function of peripheral membrane proteins (9) and protein sorting in the Golgi apparatus (10). For instance, the preference of cholesterol for ordered membranes seems to be essential for its passive transport from the endoplasmatic reticulum via the Golgi apparatus to the plasma membrane (11, 12).

Furthermore, it is still not completely clear why and how certain lipids accumulate within a cell at different locations (11). Their anchoring strength is certainly an important parameter, which to our knowledge has not yet been determined in a phase separated lipid bilayer. Therefore, determination of the dependence of anchor strength on different parameters such as the phase state of the membranes or membrane composition contributes towards understanding these important processes.

Supported lipid bilayers (SLBs) are routinely used for lipid membrane studies (13). They can be considered as a first approximation of the lipid part of cellular membranes. SLBs opened the road for the investigation of lipid membranes with sophisticated surface sensitive techniques like surface plasmon resonance (SPR) (14), total internal reflection fluorescence microscopy (TIRFM) (15), the surface force apparatus (SFA) (16) and atomic force microscopy (AFM) (17). SFA and AFM are also ideal for manipulating SLBs in a controlled way (18, 19). They have been used to extract lipids from SLBs, but relied on pulling biotinylated lipids out of a membrane and thereby having every time a different molecule and hence a different spacer length (20–22). Constant spacer length is crucial to extract thermodynamic parameters with high accuracy.

To complement bulk methods for studying the interaction between lipids and lipid membranes, we have established a single molecule based method which measures the force necessary to extract a single lipid molecule out of a lipid membrane. This provides a constant spacer length and a phase specific result. To this end, we covalently attach a single cholesterol molecule via a PEG spacer to an AFM tip. This approach guarantees that we always pull one and the same molecule out of the lipid membrane. By analyzing the extraction forces at different loading rates, we derive thermal activation parameters, such as the potential width and the lifetime of a lipid molecule in a lipid membrane. By means of molecular dynamics (MD) simulations, we are able to mimic the experiments and to describe at the molecular-level interactions between the extracted lipid and its environment.

MATERIALS AND METHODS

1,2-Dioleoyl-sn-glycero-3-phosphocholine (DOPC), 1-palmitoyl-2-oleoyl-sn-glycero-3-phosphatidylcholine (POPC), 1-palmitoyl-2-oleoyl-sn-glycero-3-phosphoethanolamine (POPE), (1,2-dioleoyl-*sn*-glycero-3-phosphocholine), sphingomyelin (SM), cholesterol and Rhodamine-PE (1,2-dioleoyl-sn-glycero-3-phosphoethanolamine-N-(lissamine rhodamine B sulfonyl)) were

purchased from Avanti Polar Lipids (Alabaster, AL). Cholesterol-PEG-NHS (5 kDa) was purchased from Nanocs (New York, NY). Methyl-PEG-NHS (6 kDa), NHS-PEG-NHS (5kDa) was from Rapp (Tuebingen, Germany). HPLC water and Hepes were purchased from Biochrom (Berlin, Germany). Chloroform (HPLC-grade) was purchased from Sigma-Aldrich (St. Louis, MO). Ethanol (pure) was obtained from Merck (Darmstadt, Germany).

Preparation of unilamellar vesicles

POPC or a mixture of DOPC, Sphingomyelin, and cholesterol (2:2:1 mol) ("PSC221 mixture") were dissolved in chloroform to a final concentration of 1 mg/mL and 0.1 mol% of Rhodamin-PE was added. The solution was filled in a glass vial and chloroform was evaporated by a nitrogen flow followed by vacuum evaporation for at least six hours at 0.1 mbar to ensure the absence of chloroform traces. Then, 1 mL of an aqueous buffer (10 mM Hepes, 4 mM $CaCl_2$) was added, and after gently shaking for 30 minutes multilamellar vesicles were obtained. To form unilamellar vesicles, the solution was extruded (Mini-Extruder, Avanti Polar Lipids) 31 times using a 100 nm filter (Nucleopore, Whatman, Piscataway, NJ) and allowed to equilibrate over night at 4°C.

Preparation of supported lipid bilayers

Supported lipid bilayers (SLBs) were formed on mica via the vesicle fusion method (23). As model lipids we chose the PSC221 mixture. To form a supported lipid bilayer the vesicles have to fuse with the surface of a mica plate (1 cm^2) that was glued into a temperature controllable fluid cell. To that aim, the vesicle solution was diluted 1 to 10 using the same buffer as before. Then, 50 µL were applied to the freshly cleaved mica sheet for an incubation time of 45 minutes. Afterwards the fluid cell was gently rinsed with 200 mL of water and incubated at 50°C for 30 minutes. After that, the fluid cell was allowed to slowly cool down to room temperature and rinsed again with at least 200 mL of pure water. Finally the quality of the bilayer was optically checked with fluorescent microscopy. If too many non-fused vesicles were present, the sample was discarded. In addition, the fluorescent image of the PSC221-SLB should display regions having either a high or a low fluorescent intensity corresponding to the liquid disordered (L_D) and the liquid ordered (L_O) state, respectively.

AFM tip functionalization

Covalent attachment of a single lipid (POPC or cholesterol) molecule (via a polyethyleneglycol (PEG) spacer) was achieved by applying the following protocol.

First silicon nitride cantilevers (MLCT, Bruker, Santa Barbara, CA) are placed in pure ethanol for 30 seconds. Chips are carefully dried with filter paper and then oxygen plasma is used to form OH-groups on the surface of the tips ('surface activation').

To form NH_2-groups on the tip surface ('amination'), chips were incubated in an APTES (amino-propyl-tri-etoxy silane)- solution (Vectabond® / dry Aceton, 1:100 v/v) for 15 minutes immediately after the activation process and were then thoroughly rinsed with aceton. The formation of stable NH_2-groups was completed by baking the chips at 70°C for 15 minutes. During baking a solution consisting of a 1 to 10 mixture of lipid-PEG-NHS/methyl-PEG-NHS (50 mg/mL) in chloroform/triethylamin (5%) was prepared. Cholesterol-functionalization of the cantilever was finally achieved by placing the cantilevers overnight in this solution in a chloroform saturated atmosphere. Right before the experiment, cantilevers were first rinsed with chloroform, then with ethanol and finally with ultrapure water.

AFM imaging and force spectroscopy

AFM imaging and force spectroscopy were performed using an MFP-3D AFM (Oxford Instruments/Asylum Research, Santa Barbara, CA). MLCT cantilevers were used for both imaging and force spectroscopy. Nominal spring constants were between 0.01 and 0.1 nN/nm and were determined by applying the thermal noise method (24, 25). Imaging was performed in intermittent contact mode, before and after performing force measurements to make sure that all extraction curves were made on the same lipid phase (Fig. 1 A, B).

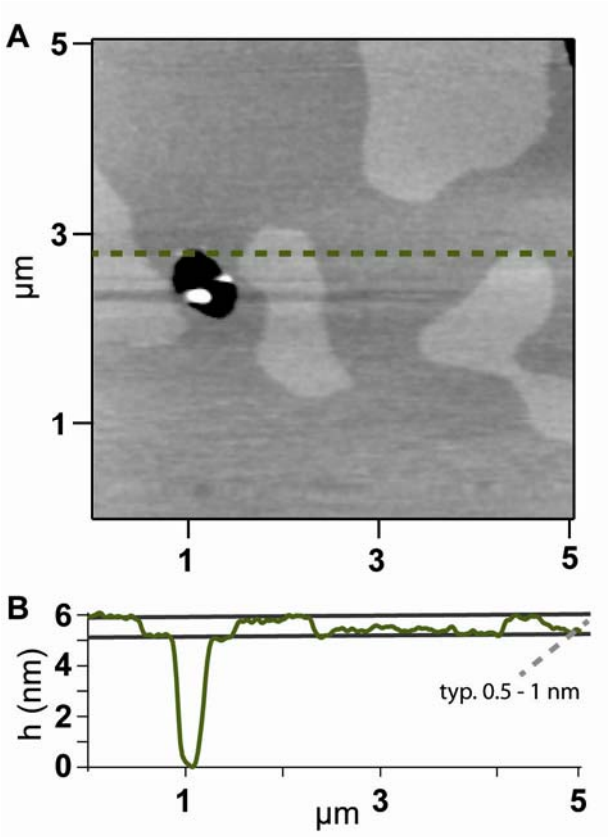

Fig. 1 (A) Tapping mode AFM image of a PSC221 membrane. The dark grey areas correspond to the L_D phase, the light grey areas correspond to the L_O phase. The black spot shows an area which is not covered by a lipid membrane. The white spot is a non fused vesicle. (B) Section corresponding to the dotted line in (A).

Extraction measurements were performed by vertically approaching the cholesterol-functionalized AFM tip towards the SLB (Fig. S1 1→2). When the tip is close to the bilayer it starts to contact the bilayer (Fig. S1 2→3). Then a small force (~100 pN) is kept constant by a feedback loop for about 4 seconds (Fig. S1 3→4). If the cholesterol inserts into the bilayer during this dwell time, it is pulled out or 'extracted' from the bilayer upon retracting the AFM tip from the bilayer (Fig. S1 4→5). The tip was moved with vertical velocities v of 50, 500 or 5000 nm/s.

Data Evaluation

Typically, all analysis steps were carried out automatically by a home-written algorithm based on the software IGOR Pro 6 (Wavemetrics, Portland, OR).

Extraction curves were first recorded as cantilever deflection versus piezo-extension. Then the cantilever sensitivity was determined by measuring the slope of the deflection-extension curve after the experiment by pressing the tip onto the hard mica surface. Together with the spring constant (see above) this allowed for calculating the force versus distance curves. The force at rupture was recorded as the extraction force. Each data point consisted of 200 to 400 extraction curves which were taken either on the liquid ordered or on the liquid disordered phase. After correction for hydrodynamic effects (26) the extraction forces were plotted in histograms for each tip velocity and either of the lipid phases.

After normalization, these probability distributions, p(f), can be directly transformed into lifetime-force distributions, τ(F), which are normally the result of constant force (force clamp) experiments. To this aim, Dudko's formula (27)

$$\tau(F) = \int_F^\infty p(f)df/(\dot{F}(F)p(F)) \qquad [1]$$

was applied where $\dot{F}(F)$ is the force dependent loading rate

$$\dot{F}(F) = v\left[\frac{1}{k} + \frac{2\beta L L_p(1+\beta F L_p)}{3+5\beta F L_p + 8(\beta F L_p)^{5/2}}\right]^{-1}. \qquad [2]$$

It was assumed that the stretching curve can be described by a worm-like-chain where L is the contour length of the linker, L_p its persistence length, $\beta = k_B T$ the thermal energy, and k is the cantilever spring constant. For the data evaluation we used L_p = 0.3 nm and L = 27 nm.

Finally, these force-dependent lifetime distributions were fitted with the Bell model

$$\tau_{Bell}(F) = \tau_{Bell}(0)e^{\frac{x_\beta F}{k_B T}} \qquad [3]$$

to get the thermal activation parameters of the lipid extraction process, namely the width of the potential x_β and the lifetime $\tau_{Bell}(0)$ at zero force ('natural lifetime'). In the following, a semi-logarithmic representation for the force-lifetime distribution was chosen because in this way the Bell model has a linear appearance.

In order to get an estimate for the activation free energy connected to the extraction process, we employed the Arrhenius law

$$\Delta G^* = -k_B T ln(A \cdot \tau_{Bell}(0)) \qquad [4]$$

where $\tau_{Bell}(0)$ is the lifetime at zero force and A is the Arrhenius prefactor. For lipids we can assume $A = 10^7$ (28).

Therefore, the ratio of the two lifetimes can be written as

$$\frac{\tau_{LO}(0)}{\tau_{LD}(0)} = \exp\left(\frac{\Delta G^*_{A,LO} - \Delta G^*_{A,LD}}{k_B T}\right) \quad [5]$$

Hence it follows for the difference between the free energies of a cholesterol molecule in both phases at zero force

$$\Delta\Delta G^* = k_B T \cdot ln \frac{\tau_{LO}(0)}{\tau_{LD}(0)} \quad [6]$$

MD Simulations

The process of lipid extraction was modeled at the atomistic level employing MD simulations. Extraction of POPE from the POPC bilayer as well as extraction of cholesterol from model L_D and L_O membranes were simulated. Both equilibrium (i.e. without pulling a POPE or cholesterol molecule out of the bilayer but with the extracted molecule equilibrated at a certain distance from the bilayer midplane) and non-equilibrium MD simulations (i.e. with pulling of POPE or cholesterol out of the bilayer) were performed. The united-atom Berger's force field was used for lipids. The L_D and L_O phases were modeled by tri-component (DOPC, SM, cholesterol) bilayers with varying ratio of the components. The L_D phase was modeled employing the DOPC:SM:cholesterol ratio of 72:48:8 while the ratio of 12:56:60 was used in the case of the L_O phase. The equilibrium free-energy profile of extracting a molecule of POPE from the POPC lipid bilayer was calculated employing potential of mean force (PMF) calculations with the umbrella sampling scheme. The force profiles of lipid extraction were calculated employing non-equilibrium simulations with the pulling of POPE and cholesterol. In the case of cholesterol extraction, a detailed evaluation of cholesterol-membrane interaction for the pulled cholesterol was performed. Additional simulations of cholesterol in L_O and L_D bilayers under equilibrium were performed to elucidate on the nature of cholesterol stabilization in both systems. Further computational details are given in the Supporting Material.

RESULTS

In order to guarantee the reliability and reproducibility of our experiments we started out by coupling phospholipids (POPE) to AFM tips and measured the force needed to extract a single POPE molecule from a POPC lipid bilayer. Fig. 2 A shows the superposition of more than 100 such extraction curves. Figs. 2 B to D show that the results within one experiment, as well as the results of different experiments with the same system are reproducible. The obtained extraction forces are 50 ±5 pN which is consistent with previous results (see discussion section).

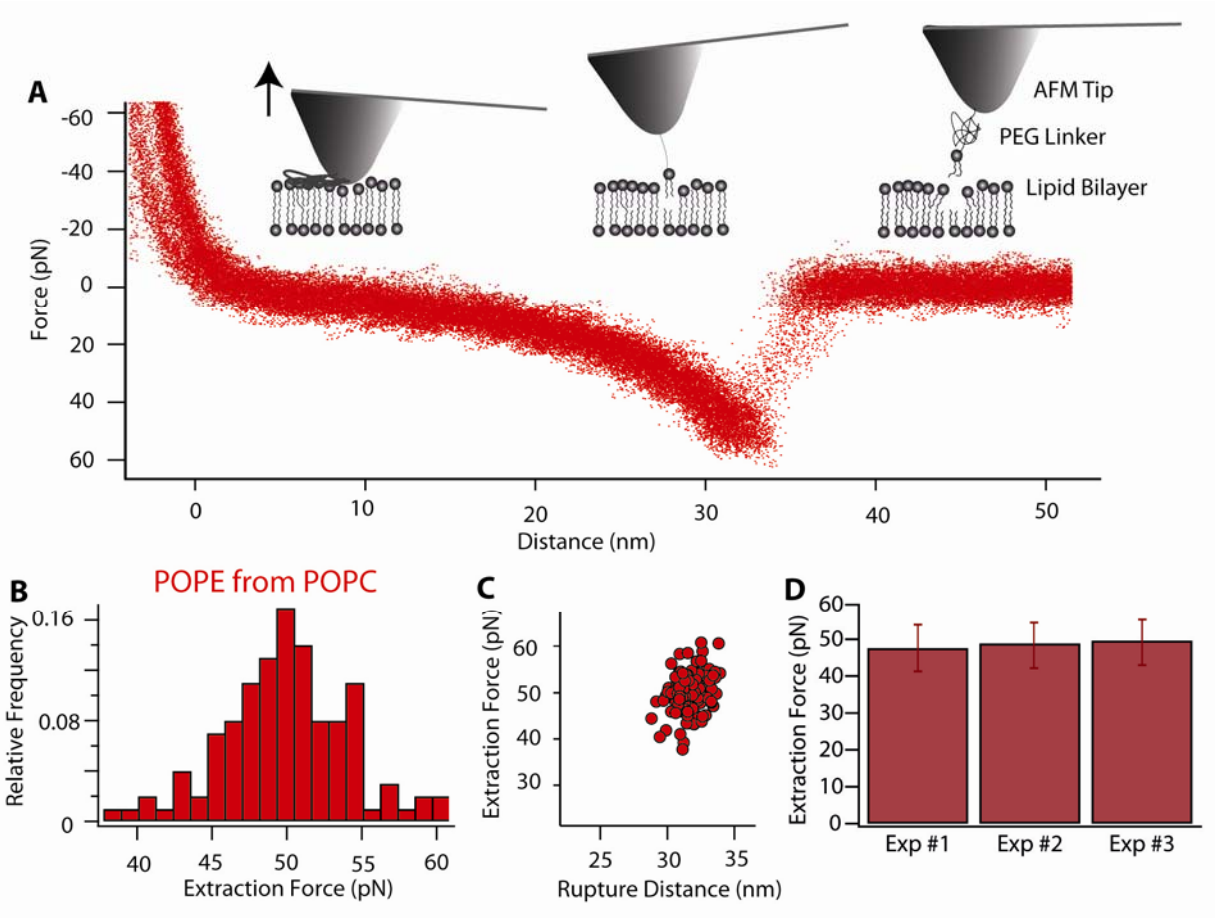

Fig. 2: Extraction of a POPE molecule from POPC bilayer at 1 µm/s. A) Superposition of more than 100 extraction curves. B) Histogram of extraction forces. C) Scatter plot of Extraction Force vs Rupture distance. D) Forces (+/- SD) needed to extract POPE molecules from POPC bilayers for three independent experiments.

In non-equilibrium MD simulations of POPE extraction from the POPC bilayer, we applied varying pulling rates between 0.0025 and 1 m/s. Rates as low as these used in the experiment cannot be achieved due to computational costs which increase with the reduction of the pulling rate. Representative force profiles are shown in Fig. 3. By comparison of the resulting non-equilibrium and equilibrium force profiles (the latter, obtained as equilibrium forces at constrained positions, approximately corresponding to an infinitely slow pulling rate), we conclude that the pulling rate of at most 0.05 m/s should be used in non-equilibrium MD simulations (see Fig. S2). The mean extraction force values are 69 and 70 (±2) pN for pulling rates of 0.0025 and 0.05 m/s, and 70 ±2 pN for the equilibrium pulling. These values are in a reasonable accord with the force obtained by the AFM experiment.

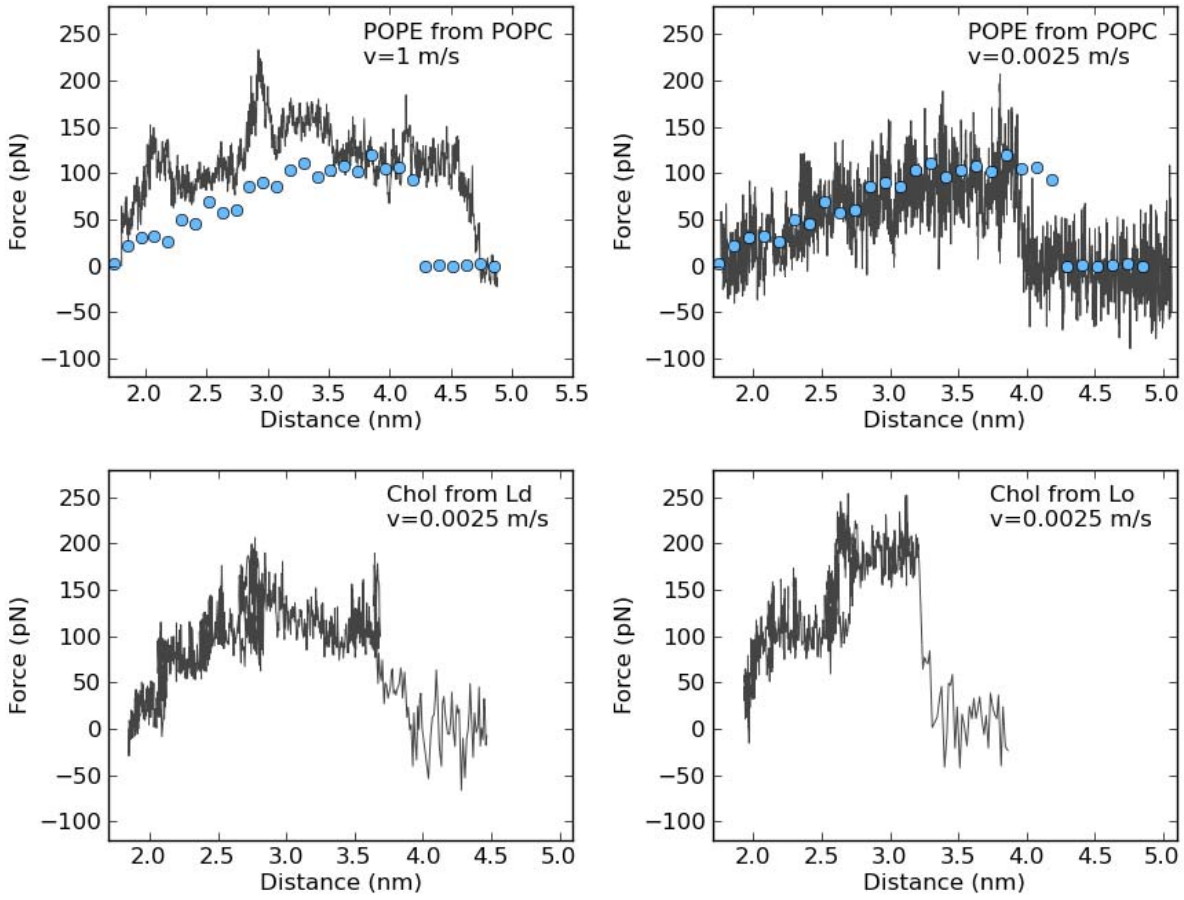

Fig. 3: Force profiles calculated during non-equilibrium MD simulations of POPE extraction from POPC (upper row) and cholesterol extraction from liquid ordered L_O and liquid disordered L_D bilayers (bottom row). For POPE, two extraction rates are depicted with the equilibrium force profile shown as blue circles. Low extraction rates (0.05 m/s at most) are required in non-equilibrium simulations to reproduce the force profile calculated under equilibrium conditions. One extraction rate is presented for cholesterol extracted from disordered and ordered lipid bilayer. The corresponding force vs time dependencies are shown in Fig. S2 in the Supporting Material.

To study the extraction of a single cholesterol molecule from a phase separated PSC221 bilayer the cholesterol molecule was attached to the AFM tip via a polyethylenglycol (PEG) spacer. Stretching curves were associated with single lipid extractions as long as the distance from the surface at the time of rupture was smaller than the contour length L of the PEG-molecule ($L \sim 27$ nm). Roughly 20 % of all force curves were identified as single extraction events. From these traces we determined the forces that were necessary to pull a single cholesterol molecule out of the liquid ordered and the liquid disordered regions of a phase separated lipid membrane made from the PSC221 mixture. In order to obtain the potential width and the lifetime, measurements were carried out with three different pulling speeds (50, 500, and 5000 nm/s) on each phase.

Fig. 4 shows representative extraction force histograms for both liquid ordered and liquid disordered phases at different pulling speeds. All measurements were carried out in duplicates and were fully reproducible. Negative controls with no cholesterol attached did not show a significant number (< 1%) of (false positive) extraction events. For the extraction of cholesterol from the L_D phase we get mean extraction forces (with standard deviation of +/- 5 pN) of 12, 20, and 30 pN for 50, 500 and 5000 nm/s, respectively. For the extraction of cholesterol from the L_O phases we get mean extraction forces (standard deviation of +/- 5 pN) of 22, 28, and 36 pN for 50, 500, and 5000 nm/s, respectively.

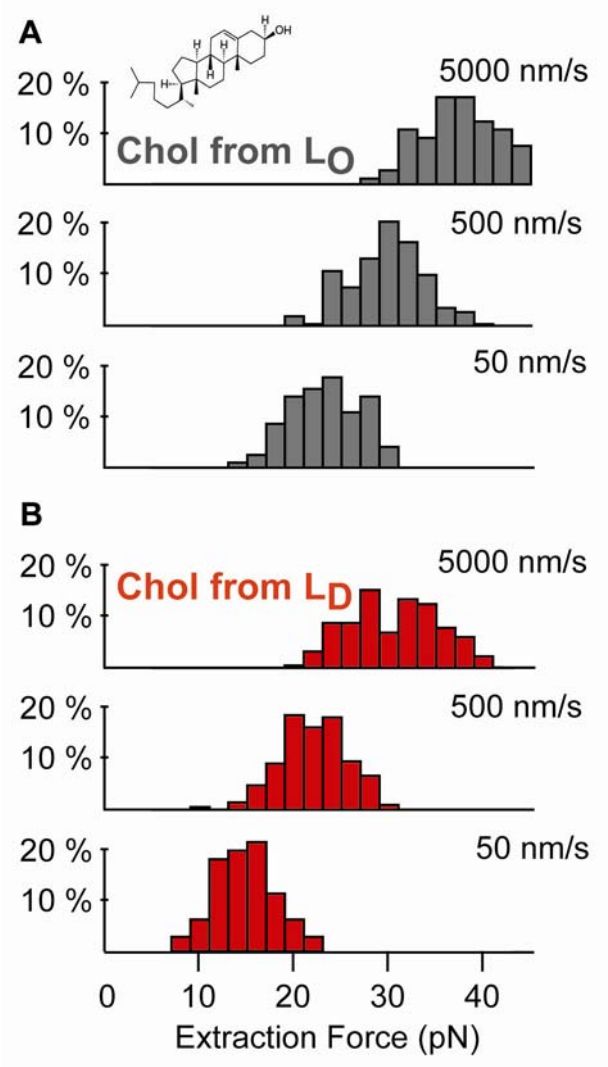

Fig. 4: Force distribution for the extraction of cholesterol from liquid ordered (L_O) phases and liquid disordered (L_D) phases. The L_O phases are rich in cholesterol, the L_D phases not.

Fig. 5 shows the measured data after model-free transformation of the histograms into force-dependent lifetimes as described in the Material and Methods. Neither the extraction from the L_O

phase nor the extraction from the L_D phase can be described with a single Bell model. Therefore, following Evans (22), we fit the data in a piecewise manner. The lifetime-force distribution for each phase is divided in a low and a high force regime and Bell models are fitted in each regime separately. The resulting thermal activation parameters are given in Table 1. Utilizing Eq. 4 and Eq. 6 results in the following activation free energies: L_O phase $\Delta G_{LO}^* = 20.6\ k_BT$ (51.5 kJ/mol); L_D phase $\Delta G_{LD}^* = 18.5\ k_BT$ (46.2 kJ/mol) and, therefore, a free energy difference between the phases of $\Delta\Delta G^*$ of 2.1 k_BT (5.2 kJ/mol).

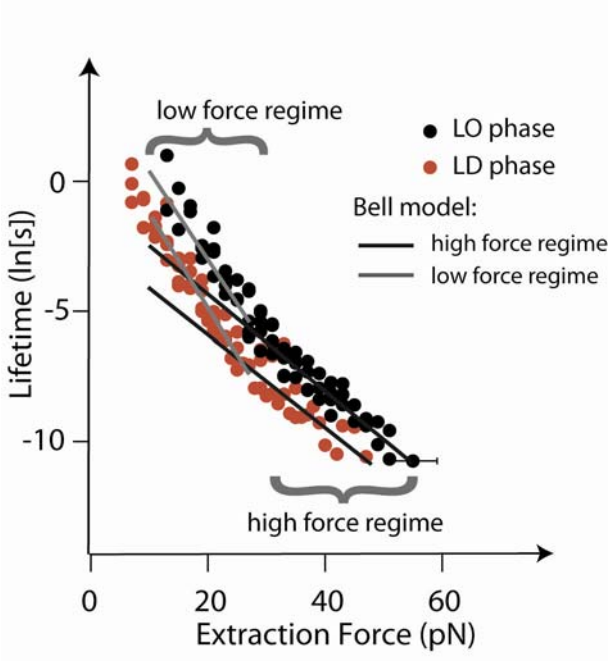

Fig. 5: Lifetime vs extraction force from the data given in Fig. 4. Both, L_O and L_D phase show a biphasic behavior, therefore a Bell model is fitted to the distributions in the high and low force regime, respectively. Forces below 10 pN are not considered because this is the sensitivity of our instrument.

	Phase State	*Potential Width* x_β	*Natural Lifetime* $\tau_{0,Bell}$
Low Force Regime	L_O	1.5 nm	90 s
	L_D	1.5 nm	11 s
High Force Regime	L_O	0.8 nm	1 s
	L_D	0.7 nm	0.1 s

Table 1 Thermal activation parameters obtained from fitting the Bell model to the low and high force regime for both the L_O and L_D phase (Fig. 5).

MD simulations of cholesterol extraction from L_O and L_D phases were performed at the pulling rates of 0.0025 and 0.05 m/s. Each value was determined from 5 independent simulations in both L_D and L_O cases with varying lateral localization of the pulled cholesterol molecule with regard to other lipid components. The resulting mean extraction force values are reported in Table 2 and representative force profiles are shown in Fig. 3 (bottom). Note that although there are minor discrepancies between the forces calculated at both pulling rates, the difference between the pulling from L_O vs. L_D phases is evident. Namely, in all simulated systems, force required for pulling cholesterol out of the membrane is higher in the L_O than that in the L_D phase. Assuming standard velocity dependence (29), the range of forces of about 90-120 pN from the MD simulation agrees well with the forces obtained from the AFM experiments. In the course of the simulations in the L_D phase, the number of contacts between the pulled cholesterol and SM increased during the pulling while contacts with DOPC became less frequent. The pulled cholesterol was also in contact with other cholesterol molecules. In L_O membranes, different possibilities were observed, as some of the cholesterol molecules resided for whole simulations either in pure sphingomyelin 'clusters' or in mixed DOPC/SM 'clusters'. We pulled cholesterol from both environments, with no differences in extraction force observed.

Pulling rate (m/s)	$F_{LO\ phase}$ ***(pN)***	$F_{LD\ phase}$ ***(pN)***
0.0025	118 (± 5)	92 (± 5)
0.05	123 (± 5)	112 (±5)

Table 2 Mean extraction force for cholesterol extraction from model L_O and L_D bilayer calculated employing non-equilibrium MD simulations.

In order to determine the molecular basis of the differences between cholesterol extraction from L_O and L_D phases, we analyzed in detail cholesterol-membrane interactions based on equilibrium MD of both types of membranes. In general, cholesterol is stabilized in lipid membranes by both polar and non-polar interactions (30). This stabilization can be characterized by numbers of contacts formed between a cholesterol molecule and molecules of lipids and water. Regarding polar interactions, three types of contacts can be observed - hydrogen bonds between 3-OH group of cholesterol and water, hydrogen bonds between 3-OH group of cholesterol and carbonyl oxygen atoms of lipid, polar pairs between 3-OH group of cholesterol and choline groups of lipids. Non-polar interactions can be quantified as close contacts between non-polar atoms of the cholesterol ring system and non-polar groups in acyl chains of lipids. Table 3 shows average numbers of H-bonds, charge pairs, and non-polar contacts formed by a cholesterol molecule in L_D and L_O bilayers. A clear effect while going from L_D to L_O phase is a significant (~9%) increase of the number of non-polar contacts, while changes of the number of polar interactions around the 3-OH group also occur. Hence, the stabilization effect for cholesterol in the L_O membrane over the L_D one is due to a combination of non-polar interactions between cholesterol and other membrane components, H-bonds, and other polar contacts.

	L_O *phase*	L_D *phase*
H-bonds	1.5 (± 0.1)	1.24 (± 0.2)
Other polar pairs	3.9 (± 0.1)	4.6 (±0.6)
Non-polar contacts	83 (± 1)	76 (± 2)

Table 3 Average number of H-bonds, charge pairs, and non-polar contacts formed by a cholesterol molecule in either the L_O or L_D phase of the lipid bilayer. Calculated with equilibrium MD simulations (i.e., without the pulling of cholesterol out of the bilayer).

Since the cholesterol is coupled to the AFM tip via its 3-OH group, we estimated to what extent this attachment geometry influences the observed differences between cholesterol extraction from L_O and L_D phases in the SLB. Based on Table 3, H-bonds which are formed by cholesterol 3-OH group change only by a fraction of a H-bond between the L_D and L_O phase in comparison with the difference of almost 10 in non-polar contacts. This suggests that the attachment of cholesterol to the AFM tip does not significantly affect the observed differences between the binding of cholesterol to L_O and L_D phases.

DISCUSSION

Cholesterol is a key component in determining the physical state of biomembranes of eukaryotic cells. In addition, cholesterol can be used as a lipid anchor e.g. for studying DNA; and its ability to modify the biophysical properties of biomembranes is used in biomimetic systems. To the best of our knowledge, this is the first study which provides insight into the forces experienced by a single cholesterol molecule when extracted from defined phases in SLBs. The general validity of our approach is tested by extracting POPE from a POPC SLB. The obtained extraction force (~50 pN) fits well with previous results (22). This is also in accord with the forces which we estimated employing MD simulations.

In the following we discuss in detail the extraction of single cholesterol molecules from a phase separated lipid bilayer. The loading rate dependent extraction forces lie between 12 and 36 pN and are therefore smaller but of the same order of magnitude as the extraction forces of phospholipids (22). In addition, this range is consistent with our non-equilibrium MD pulling simulations where we obtain forces at around 100 pN at loading rates about a factor of 10^5 higher. The measured forces show that it is more difficult to extract the cholesterol molecule from the liquid ordered phase than from the liquid disordered phase. This is also the case for the forces obtained from the MD simulations.

Further molecular information was deduced by transforming the probability distributions at different force loading rates into a force dependent lifetime distribution. The observed two regimes suggest that there is an inner and an outer barrier in the energy landscape where the width of the outer barrier should in this case correspond to the full length of the molecule (22). Indeed, the obtained value corresponds well with the full length of the cholesterol molecule (~1.6 nm).

Forces of 25 pN and above could cause a deformation of the energy landscape in such a way that now the inner barrier becomes the dominating one, resulting in a change of the slope of the fit in

Fig. 5. The location of the inner barrier (i.e. the width of the inner potential) agrees, very well with the length of cholesterols iso-octyl-group (~0.7 nm) (see Fig. 6).

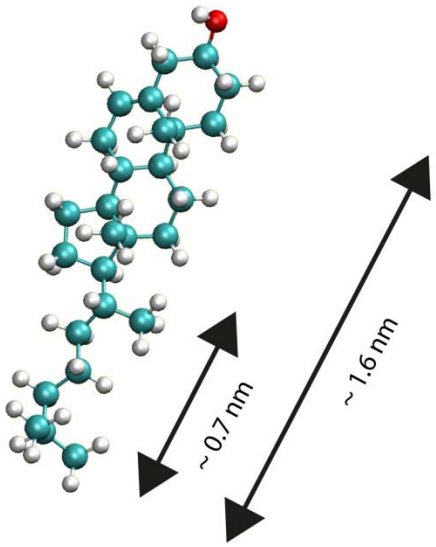

Fig. 6: The length of a cholesterol molecule is roughly 1.6 nm. The length of its iso-octyl part is about 0.7 nm. Interestingly, these dimensions match the widths of the full potential and the widths of the inner potential obtained from the Bell model (Fig. 5). The polyethylengylcol (which links the cholesterol to the AFM tip) is attached to the oxygen atom of the 3-OH group (depicted in red).

The Bell model also directly yields natural lifetimes, i.e. the time the cholesterol molecule would stay on average in the lipid bilayer at zero force. A comparison for the two lipid phases (L_O and L_D) shows that the cholesterol lifetime in the L_O phase is roughly 10 times higher than in the L_D phase for both regimes (see Table 1). Other experiments with lipid membranes show the same trends in different lipid phases. For example, in one study the lifetime of cholesterol was estimated to be 38 h on (saturated) sphingomyelin vesicles and 4 h on unsaturated di-acyl-phospholipids (31). Similarly, cell membranes, which were exposed to an efficient cholesterol acceptor (Cyclodextrin) showed two kinetic pools: one with a half lifetime of 20 minutes and the other of 20 seconds (32). These results are consistent with the concept of microdomains (slow pool, L_O phase) which are surrounded by the rest of the plasma membrane (fast pool, L_D phase). Thus, our ratio for the cholesterol lifetime in L_O and L_D phase is consistent with measurements made by others.

Since the obtained lifetime of 90 s for the whole cholesterol molecule (in the low force regime) in the cholesterol rich L_O phase seems to be relatively low, we compare it with the situation in cholesterol micelles. To that end, we use an approximation from Israelchivilli (28) to calculate a critical micelle concentrations (*CMC*):

$$CMC \approx 55 \frac{\tau_{collision}}{\tau_{residence}} \qquad [7]$$

Here, the residence time $\tau_{residence}$ corresponds to the mean lifetime in our experiments and the collision time $\tau_{collision}$ corresoponds to a typical motional correlation time, which is on the order of $10^{-7}s$ for lipids (28).

Inserting our measured lifetime from the low force regime (Fig. 5) for the cholesterol rich L_O phase into Eq. 7 results in

$$CMC_{LO} \approx 55\frac{10^{-7}s}{90\ s}[M] \approx 60\ nM \quad [8]$$

This corresponds well to the value of 25 - 40 nM which was measured in (33) for the CMC of cholesterol with micelles. Thus, thermodynamic parameters from micelles and SLBs seem to be rather similar to each other.

MD simulations help to exclude the possibility that our attachment geometry (where PEG is linked to the 3-OH group) changes the measured lifetimes significantly, because they show that there's only a minor change in the number of polar interactions around the 3-OH group (where the linker is attached - see Fig. 6). Furthermore, the simulations suggest that the preference of cholesterol for the lipid ordered phase over the lipid disordered phase arises from non-polar interactions between cholesterol and other membrane components. This is evidenced by a significant (~9%) increase of the number of non-polar contacts with the change from L_D to L_O phase.

Independent on which molecular interaction is mainly responsible for the increased affinity of the cholesterol for the L_O phase, it results in a higher cholesterol concentration in the L_O phase than in the L_D phase and also in a difference for the desorption energies in the two phases. Therefore, it is interesting to compare this difference in desorption energies with the difference in the free energies which corresponds to the respective concentrations in the phases. Assuming that the cholesterol concentrations in both phases are in equilibrium and further assuming that cholesterol concentrations can be used instead of the activities, one can calculate this difference in the free energies from the ratio of the two concentrations by invoking the mass action law (28).

$$\Delta G = k_B T ln\frac{[Chol]_{LO}}{[Chol]_{LD}} \quad [9]$$

We use the Gibb's phase diagram in (34) to obtain an estimate for the ratio $[Chol]_{LO}$ / $[Chol]_{LD}$ of 47/7. In this way we get

$$\Delta G = k_B T \cdot ln\frac{47}{7} = 1.9\ k_B T\ (4.7\ kJ/mol) \quad [10]$$

This is again consistent with the difference in the activation free energies based on the ratio of the lifetimes of the two phases, namely 2.1 k_BT (5.2 kJ/mol).

CONCLUSION

We have designed and carried out an AFM force spectroscopic experiment to determine the anchorage strength of a single cholesterol molecule in the liquid ordered and liquid disordered phases of a phase separated lipid bilayer made from a tertiary lipid mixture. Loading rate dependent measurements with a constant linker length allow comparing extraction force, unloading lifetime, the width of the Bell potential, and the interaction free energy for the different phases. These phases could be imaged by AFM in advance. In that way a direct correlation of topographic features (i.e., the L_D- and the L_O phase) with force data becomes feasible.

As expected, the extraction forces for the L_O phase are significantly higher than for the L_D phase, but overall the estimated lifetimes come out rather short (tens of seconds). We have therefore supported our findings with a thorough energetic discussion and comparison with the CMC of similar systems as well as with equilibrium and non-equilibrium (pulling) MD simulations. The MD simulations in addition show that the main difference of cholesterol interaction with the L_O and L_D phase is due to changes in non-polar contacts. Our experiments constitute an important step toward understanding microdomain formation and stability. We anticipate that this method will be extended towards protein lipid interactions.

ACKNOWLEDGEMENTS

The authors thank Erich Sackmann (TU Munich) for helpful discussions, the SFB863, the Hanns-Seidel-Stiftung (HSS), and the ESF EuroMEMBRANE CRP OXPL (Hu 997/7-1) for financial support. PJ thanks the Czech Science Foundation (grant P208/12/G016) and acknowledges the Academy of Sciences of the Czech Republic for the Praemium Academie award and the Academy of Finland for the Finland Distinguished Professor (FiDiPro) award.

REFERENCES

1. Hancock, J.F. 2006. Lipid rafts: contentious only from simplistic standpoints. Nat. Rev. Mol. Cell Biol. 7: 456–62.

2. Pike, L.J. 2006. Rafts defined: a report on the Keystone Symposium on Lipid Rafts and Cell Function. J. Lipid Res. 47: 1597–8.

3. Lingwood, D., and K. Simons. 2010. Lipid rafts as a membrane-organizing principle. Science. 327: 46–50.

4. Simons, K., and R. Ehehalt. 2002. Cholesterol , lipid rafts , and disease. J Clin Invest. 110: 597–603.

5. Veatch, S.L., and S.L. Keller. 2005. Seeing spots: complex phase behavior in simple membranes. Biochim. Biophys. Acta. 1746: 172–85.

6. De Almeida, R.F.M., A. Fedorov, and M. Prieto. 2003. Sphingomyelin/phosphatidylcholine/cholesterol phase diagram: boundaries and composition of lipid rafts. Biophys. J. 85: 2406–16.

7. Pandit, S. a, S. Vasudevan, S.W. Chiu, R.J. Mashl, E. Jakobsson, et al. 2004. Sphingomyelin-cholesterol domains in phospholipid membranes: atomistic simulation. Biophys. J. 87: 1092–100.

8. Lev, S. 2010. Non-vesicular lipid transport by lipid-transfer proteins and beyond. Nat. Rev. Mol. Cell Biol. 11: 739–50.

9. Cross, B., F. Ronzon, B. Roux, and J.-P. Rieu. 2005. Measurement of the anchorage force between GPI-anchored alkaline phosphatase and supported membranes by AFM force spectroscopy. Langmuir. 21: 5149–53.

10. Sprong, H., P. Van Der Sluijs, and G. Van Meer. 2001. How proteins move lipids and lipids move proteins. 2: 504–513.

11. Bennett, W.F.D., and D.P. Tieleman. 2012. Molecular simulation of rapid translocation of cholesterol, diacylglycerol, and ceramide in model raft and nonraft membranes. J. Lipid Res. 53: 421–9.

12. Meer, G. Van, D. Voelker, and G. Feigenson. 2008. Membrane lipids: where they are and how they behave. Nat. Rev. Mol. …. 9: 112–124.

13. Sackmann, E. 1996. Supported membranes: scientific and practical applications. Science. 271: 43–8.

14. Besenicar, M., P. Macek, J.H. Lakey, and G. Anderluh. 2006. Surface plasmon resonance in protein-membrane interactions. Chem. Phys. Lipids. 141: 169–78.

15. Oreopoulos, J., R.F. Epand, R.M. Epand, and C.M. Yip. 2010. Peptide-induced domain formation in supported lipid bilayers: direct evidence by combined atomic force and polarized total internal reflection fluorescence microscopy. Biophys. J. 98: 815–23.

16. Benz, M., T. Gutsmann, N. Chen, R. Tadmor, and J. Israelachvili. 2004. Correlation of AFM and SFA measurements concerning the stability of supported lipid bilayers. Biophys. J. 86: 870–9.

17. Milhiet, P.-E., F. Gubellini, ..., and D. Lévy. 2006. High-resolution AFM of membrane proteins directly incorporated at high density in planar lipid bilayer. Biophys. J. 91: 3268–75.

18. Stetter, F.W.S., and T. Hugel. 2013. The Nanomechanical Properties of Lipid Membranes are Significantly Influenced by the Presence of Ethanol. Biophys. J. 104: 1049–1055.

19. Clausen-Schaumann, H., M. Seitz, R. Krautbauer, and H.E. Gaub. 2000. Force spectroscopy with single bio-molecules. Curr. Opin. …. : 524–530.

20. Wieland, J. a, A. a Gewirth, and D.E. Leckband. 2005. Single-molecule measurements of the impact of lipid phase behavior on anchor strengths. J. Phys. Chem. B. 109: 5985–93.

21. Ounkomol, C., H. Xie, P. a Dayton, and V. Heinrich. 2009. Versatile horizontal force probe for mechanical tests on pipette-held cells, particles, and membrane capsules. Biophys. J. 96: 1218–31.

22. Evans, E., and F. Ludwig. 2000. Dynamic strengths of molecular anchoring and material cohesion in fluid biomembranes. J. Phys. Condens. Matter. 12: A315–A320.

23. Leonenko, Z. V, A. Carnini, and D.T. Cramb. 2000. Supported planar bilayer formation by vesicle fusion: the interaction of phospholipid vesicles with surfaces and the effect of gramicidin on bilayer properties using atomic force microscopy. Biochim. Biophys. Acta. 1509: 131–47.

24. Sader, J.E., I. Larson, P. Mulvaney, and L.R. White. 1995. Method for the calibration of atomic force microscope cantilevers. Rev. Sci. Instrum. 66: 3789–3798.

25. Pirzer, T., and T. Hugel. 2009. Atomic force microscopy spring constant determination in viscous liquids. Rev. Sci. Instrum. 79: 035110.

26. Alcaraz, J., L. Buscemi, and M. Puig-de-Morales. 2002. Correction of microrheological measurements of soft samples with atomic force microscopy for the hydrodynamic drag on the cantilever. Langmuir. : 716–721.

27. Dudko, O.K., G. Hummer, and A. Szabo. 2008. Theory, analysis, and interpretation of single-molecule force spectroscopy experiments. Proc. Natl. Acad. Sci. U. S. A. 105: 15755–60.

28. Israelachvili, J.N. 2010. Intermolecular and Surface Forces: With Applications to Colloidal and Biological Systems (Colloid Science). 3rd ed. Academic Press.

29. Evans, E., and K. Ritchie. 1997. Dynamic strength of molecular adhesion bonds. Biophys. J. 72: 1541–55.

30. Róg, T., M. Pasenkiewicz-Gierula, I. Vattulainen, and M. Karttunen. 2009. Ordering effects of cholesterol and its analogues. Biochim. Biophys. Acta. 1788: 97–121.

31. Kan, C.C., R. Bittman, and J. Hajdu. 1991. Phospholipids containing nitrogen- and sulfur-linked chains: kinetics of cholesterol exchange between vesicles. Biochim. Biophys. Acta. 1066: 95–101.

32. Haynes, M.P., M.C. Phillips, and G.H. Rothblat. 2000. Efflux of cholesterol from different cellular pools. Biochemistry. 39: 4508–17.

33. Haberland, M.E., and J. a Reynolds. 1973. Self-association of cholesterol in aqueous solution. Proc. Natl. Acad. Sci. U. S. A. 70: 2313–6.

34. Smith, A.K., and J.H. Freed. 2009. Determination of Tie-Line Fields for Coexisting Lipid Phases: An ESR Study †. J. Phys. Chem. B. 113: 3957–3971.

35. Hess, B., C. Kutzner, D. ven der Spoel, and E. Lindhal. 2008. GROMACS 4: Algorithms for Highly Efficient, Load-Balanced, and Scalable Molecular Simulation. J. Chem. Theory Comput. 4: 435–447.

36. Kumar, S., J.M. Rosenberg, D. Bouzida, R.H. Swendsen, and P.A. Kollman. 1992. THE weighted histogram analysis method for free-energy calculations on biomolecules. I. The method. J. Comput. Chem. 13: 1011–1021.

37. Berger, O., and O. Edholm. 2002. Molecular Dynamics Simulations of a Fluid Bilayer of Dipalmitoylphosphatidylcholine at Full Hydration, Constant Pressure, and Constant Temperature. Biophys. J. 72: 2002–2013.

38. Berendsen, H.J.C., J.P.M. Postma, W.F. Van Gunsteren, and J. Hermans. 1981. Interaction Models for Water in Relation to Protein Hydrati on. In: Intermolecular Forces. Dordrecht: D. Reidel Publishing Company. pp. 331–342.

39. Parrinello, M., and A. Rahman. 1981. Polymorphic transitions in single crystals: A new molecular dynamics method. J. Appl. Phys. 52: 7182.

40. Nose, S. 1984. A molecular dynamics method for simulations in the canonical ensemble. Mol. Phys. 52: 255–268.

41. Essmann, U., L. Perera, M.L. Berkowitz, T. Darden, H. Lee, et al. 1995. A smooth particle mesh Ewald method. J. Chem. Phys. 103: 8577.

42. Hess, B., H. Bekker, H.J.C. Berendsen, and J.G.E.M. Fraaije. 1997. LINCS: A linear constraint solver for molecular simulations. J. Comput. Chem. 18: 1463–1472.

43. Hockney, R.., S.. Goel, and J.. Eastwood. 1974. Quiet high-resolution computer models of a plasma. J. Comput. Phys. : 148–158.

44. Schwierz, N., D. Horinek, S. Liese, T. Pirzer, B.N. Balzer, et al. 2012. On the relationship between peptide adsorption resistance and surface contact angle: a combined experimental and simulation single-molecule study. J. Am. Chem. Soc. 134: 19628–38.

Supporting Material

MD Simulations Methodology

The force related to extraction of POPE and cholesterol molecules from lipid bilayers was calculated employing classical molecular dynamics simulations. Calculations were performed with Gromacs 4.5.1 software (double precision compilation) (1) The potential of mean force (PMF) computation scheme with umbrella sampling and the weighted histogram analysis method (WHAM) were employed (2). In the case of POPE extraction from the POPC bilayer, the membrane built of 63 POPC and 1 POPE lipids was hydrated with over 5000 molecules of water. The empirical united-atom Berger force field was employed for lipid molecules while water molecules were described with the simple-point charge model (3, 4). Simulations were performed in the NPT ensemble. A 4.6×4.6×11.6 nm simulation box was used with periodic boundary conditions employed. The pressure was controlled with the use of the semiisotropic Parrinello-Ramhan barostat with the pressure of 1 bar (5). The temperature of 310 K was controlled by the Nose-Hoover thermostat (6). Nonbonded interactions were accounted for employing a cutoff of 1 nm, with the particle mesh Ewald method used for calculation of long-range electrostatic forces (7). Bond lengths in lipids were constrained with the LINCS algorithm, and water molecules were kept rigid using the SETTLE algorithm (8, 9). A time step of 2 fs was employed for integration of equations of motion.

We started with a 30 ns equilibration of the system followed by a generation of initial configurations for umbrella sampling by pulling the nitrogen atom of the POPE headgroup along the normal to the membrane (z-coordinate). For pulling, an umbrella potential with a force constant of 1000 kJ mol^{-1} nm^{-2} was employed with the pulling rate of 0.002 nm ps^{-1}. 35 initial configurations were chosen with a spacing of 0.1 nm in the position of the nitrogen atom with respect to the center of mass of the bilayer. For each of such umbrella sampling windows the z-coordinate of the nitrogen atom was restrained with a force constant of 3000 kJ $mol^{-1}nm^{-2}$ and 10 ns equilibration runs were performed, each followed by a further 10 ns production run. For each umbrella sampling window the values of the force acting on the restrained nitrogen atom of POPE in the z-direction during the production run were collected. The WHAM method was then employed for calculating the potential of mean force, i.e., the changes of the free energy.

In the case of cholesterol, we simulated non-equilibrium pulling of single cholesterol molecules from lipid bilayers that were mimicking L_O and L_D membrane phases. The following lipid compositions were employed: DOPC:SM:chlesterol = 12:56:60 (L_O phase), DOPC:SM:cholesterol = 72:48:8 (L_D phase). The bilayers consisted of 128 lipids hydrated with over 6000 water molecules. Temperature was equal to 300 K in all cases. As, in particular, the L_O system is expected to exhibit lateral inhomogeneities, some of the pulling trajectories were repeated with different cholesterol molecules being pulled. All remaining simulation parameters were the same as in the case of the POPE/POPC simulations.

Interactions of cholesterol with lipids were studied in equilibrium MD simulations, i.e. without pulling cholesterol out of the bilayer (trajectories of 100 ns-length were calculated, last 50 ns were used for analysis). All H-bonds formed by 3-OH group of cholesterol and carbonyl oxygen atoms of both DOPC and SM lipids, as well as hydrogen bonds formed between 3-OH and water

were taken into account. No cholesterol-cholesterol H-bonds were observed in simulations. The donor–acceptor cut-off of 0.325 nm and angle cut-off of 35˚ were employed for H-bond definition. Charge pairs were defined with a cut-off of 0.45 nm between 3-OH oxygen and carbon atoms in DOPC and SM headgroups. Non-polar contacts are defined with a cut-off of 0.8 nm between carbon atoms of cholesterol and carbon atoms of DOPC, SM, and other cholesterol molecules. The cut-offs match first minima in corresponding radial distribution functions. Both H-bonds and charge pairs are given per cholesterol molecule, and non-polar contacts are given per carbon atom of cholesterol. Numbers of contacts and H-bonds were calculated as average values along the equilibrated MD trajectories. Error values were estimated from corresponding standard deviations.

Calculated forces were depicted in Fig. 3 as force profiles corresponding to the experimental extraction profiles, i.e., the puling force was shown as the function of the distance of the pulled molecule from the bilayer midplane. This distance is oscillating along the pulling trajectory due to the finite force constant employed for extraction. Hence, the distances in Fig. 3 were averaged using the moving average procedure. The original force vs time dependencies are shown in Fig. S2. The values of the mean extraction force were calculated as mean force required for extracting a lipid from a bilayer along the whole pulling process (similarly to (10)). For POPE pulling, the error of the calculated mean force was estimated from standard deviation of the mean force calculated for statistically independent subsets of data. In the case of cholesterol pulled out from both L_O and L_D membrane phases, the mean extraction force was calculated as an average from five independent puling trajectories and the errors were estimated from standard deviation.

FIGURE S1

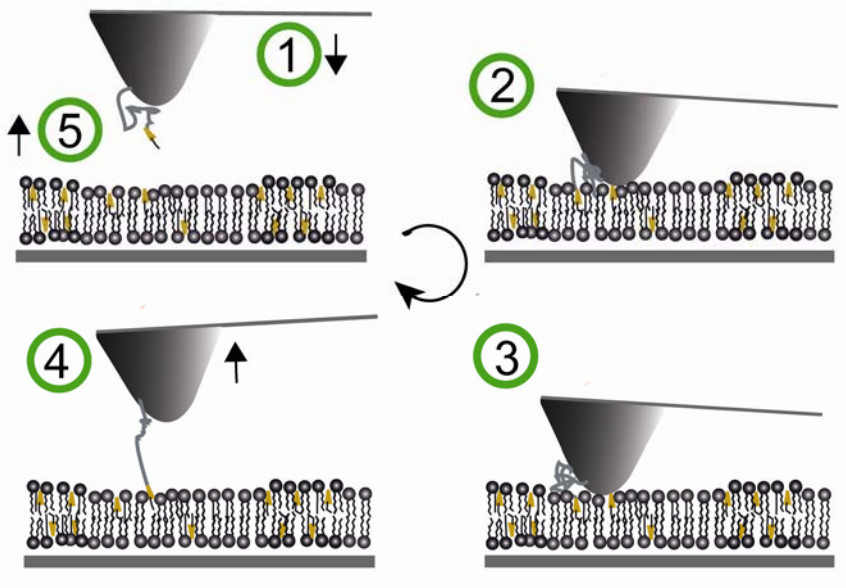

Fig. S1: Schematic representation of the single molecule extraction process. Extraction measurements were performed by vertically approaching the cholesterol-functionalized AFM tip towards the SLB (1→2). When the tip is close to the bilayer it starts to contact the bilayer

(2→3). Then a small force (~100 pN) is kept constant by a feedback loop for about 4 seconds (3→4). If the cholesterol inserts into the bilayer during this dwell time, it is pulled out or 'extracted' from the bilayer upon retracting the AFM tip from the bilayer (4→5).

FIGURE S2

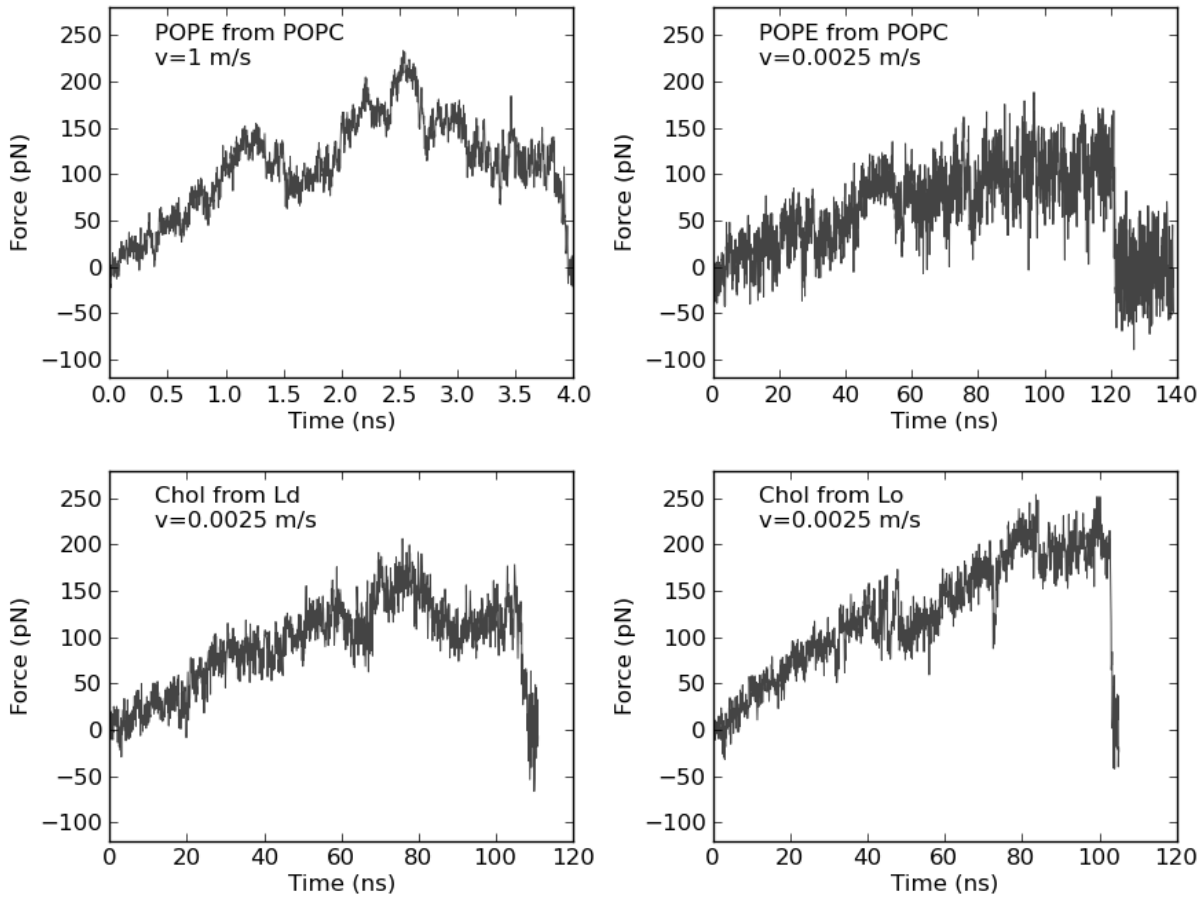

Fig. S2: Force vs time dependencies calculated during non-equilibrium MD simulations of POPE extraction from POPC (upper row) and cholesterol extraction from L_O and L_D bilayers (bottom row). These profiles correspond to the force profiles shown in Fig. 3 (main text).

Supporting References

1. Hess, B., C. Kutzner, D. ven der Spoel, and E. Lindhal. 2008. GROMACS 4: Algorithms for Highly Efficient, Load-Balanced, and Scalable Molecular Simulation. J. Chem. Theory Comput. 4: 435–447.

2. Kumar, S., J.M. Rosenberg, D. Bouzida, R.H. Swendsen, and P.A. Kollman. 1992. THE weighted histogram analysis method for free-energy calculations on biomolecules. I. The method. J. Comput. Chem. 13: 1011–1021.

3. Berger, O., and O. Edholm. 2002. Molecular Dynamics Simulations of a Fluid Bilayer of Dipalmitoylphosphatidylcholine at Full Hydration, Constant Pressure, and Constant Temperature. Biophys. J. 72: 2002–2013.

4. Berendsen, H.J.C., J.P.M. Postma, W.F. Van Gunsteren, and J. Hermans. 1981. Interaction Models for Water in Relation to Protein Hydrati on. In: Intermolecular Forces. Dordrecht: D. Reidel Publishing Company. pp. 331–342.

5. Parrinello, M., and A. Rahman. 1981. Polymorphic transitions in single crystals: A new molecular dynamics method. J. Appl. Phys. 52: 7182.

6. Nose, S. 1984. A molecular dynamics method for simulations in the canonical ensemble. Mol. Phys. 52: 255–268.

7. Essmann, U., L. Perera, M.L. Berkowitz, T. Darden, H. Lee, et al. 1995. A smooth particle mesh Ewald method. J. Chem. Phys. 103: 8577.

8. Hess, B., H. Bekker, H.J.C. Berendsen, and J.G.E.M. Fraaije. 1997. LINCS: A linear constraint solver for molecular simulations. J. Comput. Chem. 18: 1463–1472.

9. Hockney, R.., S.. Goel, and J.. Eastwood. 1974. Quiet high-resolution computer models of a plasma. J. Comput. Phys. : 148–158.

10. Schwierz, N., D. Horinek, S. Liese, T. Pirzer, B.N. Balzer, et al. 2012. On the relationship between peptide adsorption resistance and surface contact angle: a combined experimental and simulation single-molecule study. J. Am. Chem. Soc. 134: 19628–38.